



Submit a Revision

Respond to the reviewers' comments by entering text into the text boxes provided. [Read More ...](#)

1 [View and Respond to Decision Letter](#)

Save and Continue

✓ 2 [Type, Title, & Abstract](#)

Decision Letter

✓ 3 [Attributes](#)

Wageningen, December 1, 2014

✓ 4 [Authors & Institutions](#)

MPP-OA-14-274

"The *Penicillium digitatum* protein O-Mannosyltransferase Pmt2 is required for cell wall integrity, conidiogenesis, virulence and sensitivity to the antifungal peptide PAF26"

5 [Details & Comments](#)

Harries, Eleonora; Gandía, Mónica; Carmona, Lourdes; Marcos, Jose F.

✓ 6 [File Upload](#)

Dear Dr. Marcos,

7 [Review & Submit](#)

Thank you for submitting your manuscript to Molecular Plant Pathology. It has now been reviewed and the comments of the reviewer(s) are included at the bottom of this letter.

The reviewer(s) have recommended publication, but also suggest some minor revisions which I believe would improve your manuscript. Therefore, I invite you to respond to the reviewer(s)' comments and submit a revised version of your manuscript.

Please use the link below to submit your revision

https://mc.manuscriptcentral.com/mpp?URL_MASK=e1f672fad1434c6da1add0d06654879a

Your manuscript number will be appended to denote a revision.

You are unable to make revisions to the original version of the manuscript. Instead, please create a new version and highlight the changes within your manuscript by using the track changes mode in MS Word or by using bold or coloured text.

Once the revised manuscript is prepared, you can upload it and submit it through your Author Center.

IMPORTANT: Your original files are available to you when you upload your revised manuscript. Please delete any redundant files before completing the submission.

When submitting your revised manuscript, you will be able to respond to the comments made by the reviewer(s) in the space provided. You can use this space to document any changes you make to the original manuscript.

In order to expedite the processing of the revised manuscript, please be as specific as possible in your response to the reviewer(s).

At Molecular Plant Pathology we try to minimise the time between submission and publication. Your revised manuscript should be resubmitted as soon as possible. If you are unable to submit your revision in a reasonable amount of time, we may have to consider your paper as a new submission.

Once again, thank you for submitting your manuscript to Molecular Plant Pathology and I look forward to receiving your revision.

Sincerely,

Gert HJ Kema

Senior Editor, Molecular Plant Pathology
gert.kema@wur.nl

Reviewer(s)' comments:
Referee: 1

Comments to the Author

The current work is aimed at identification and characterization the function of pmt genes in *Penicillium digitatum* as far as its effect on cell wall integrity, morphogenesis, virulence and sensitivity to anti-fungal protein PAF26.

Overall, this work is very well written and results are presented adequately. The findings are very interesting and shed light on the role of protein O-Mannosyltransferase in the biology of *P. digitatum*. Except for minor comments, mainly in the material and methods sections, that are indicated directly in the text, this reviewers finds the manuscript in good shape and recommend its acceptance.

Referee: 2

Comments to the Author

This work shows the effect of PMT genes of *Penicillium digitatum*, specifically *pmt2*, on fungal growth and virulence on citrus fruit.

The subject is quite original and the information obtained could be useful for a future management of this disease by using antifungal peptide as PAF26. This basic research provides new and interesting information to understand the role of some of these Pmts on virulence factor of fungal postharvest pathogens. The structure is consistent with that required by the journal.

In general, the methodology is appropriate and can achieve the objectives of the work. However, some sections are explaining too much details (construction of plasmids vector, transformation, ...) and other not enough (Infection assays: variety of oranges? Harvest season? Quality parameter of fruit? Many works on fruit have demonstrated the importance of quality parameter of fruit to evaluate the pathogenicity of postharvest diseases. How did you make wounds? How did you evaluate conidiation index? Statistical analysis to virulence assays: Show mean \pm SD is not enough (fig 7)!


In general, results are well presented and maintain a logical and appropriate sequence. However, statistical analysis is not rather adequate; For example, from relative expression results obtained in Fig 3 you chose *pmt2* to continue your work; however the relative expression of both *pmt2* and *pmt4* at 4 pdi in (A) experiment is equal, but this behaviour was not repeated at (B) experiment. Do you believe that from these results is consistent enough to continue your study only with *pmt2* and not *pmt4*?


The discussion can take advantage of all the results obtained by you and achieve a good discussion related to the experience of other authors.

The manuscript is generally well written, with prior literature cited and discussed extensively and appropriately.

Only some minor aspects such as some aspects on statistical analyses and additional information on experimental procedures will be needed.

Respond to these comments

 Response to Decision Letter

 Save and Continue

© Thomson Reuters | © ScholarOne, Inc., 2014. All Rights Reserved.

ScholarOne Manuscripts and ScholarOne are registered trademarks of ScholarOne, Inc.

ScholarOne Manuscripts Patents #7,257,767 and #7,263,655.

 @ScholarOneNews |  System Requirements |  Privacy Statement |  Terms of Use



The *Penicillium digitatum* protein O-Mannosyltransferase Pmt2 is required for cell wall integrity, conidiogenesis, virulence and sensitivity to the antifungal peptide PAF26

Journal:	<i>Molecular Plant Pathology</i>
Manuscript ID:	MPP-OA-14-274
Manuscript Type:	Original Article
Date Submitted by the Author:	29-Oct-2014
Complete List of Authors:	Harries, Eleonora; IATA-CSIC, Gandía, Mónica; IATA-CSIC, Carmona, Lourdes; IATA-CSIC, Marcos, Jose F.; IATA-CSIC,
Keywords:	<i>Penicillium digitatum</i> , protein glycosylation, postharvest decay, citrus fruit, cell wall, antifungal peptides

1
2
3 **The *Penicillium digitatum* protein O-Mannosyltransferase Pmt2**
4 **is required for cell wall integrity, conidiogenesis, virulence and**
5 **sensitivity to the antifungal peptide PAF26.**
6
7
8
9

10
11
12
13
14
15 ELEONORA HARRIES[§], MÓNICA GANDÍA, LOURDES CARMONA,

16
17
18 AND JOSE F. MARCOS*
19

20
21
22
23 Departamento de Ciencia de los Alimentos, Instituto de Agroquímica y
24 Tecnología de Alimentos (IATA), CSIC. Avda. Agustín Escardino-7. Paterna.
25
26 46980 Valencia. Spain
27

28
29
30 [§]*Present address:* Laboratorio de Sanidad Vegetal, CONICET - EEA INTA
31 Salta. Ruta Nacional 68 km 172 (4403) Cerrillos. Salta. Argentina
32
33

34
35 **To whom correspondence should be sent:* Dr. Jose F. Marcos. IATA-CSIC.
36 Avenida Agustín Escardino - 7. Paterna. 46980 Valencia. Spain. e-mail:
37 jmarcos@iata.csic.es. Tel: (34)963.900.022.
38
39
40
41
42
43
44

45 **Running title:** *P. digitatum* protein glycosylation and virulence
46

47 **Keywords:** *Penicillium digitatum*, protein glycosylation, postharvest decay,
48 citrus fruit, cell wall, antifungal peptides.
49
50

51
52
53 **Word Count** (Title, References and Supporting material not included): 6,998
54
55
56
57
58
59
60

1 SUMMARY

2 The activity of protein O-mannosyltransferases (Pmt) affects the
3 morphogenesis and virulence of fungal pathogens. *PMT* genes have been
4 recently shown to determine the sensitivity of *Saccharomyces cerevisiae* to the
5 antifungal peptide PAF26. This study reports the identification and
6 characterisation of the three *Pdpmt* genes in the citrus postharvest pathogen
7 *Penicillium digitatum*. The *Pdpmt* genes are expressed during fungal growth
8 and fruit infection, with the highest induction for *Pdpmt2*. *Pdpmt2* complemented
9 the growth defect of the *S. cerevisiae* $\Delta pmt2$ strain. The *Pdpmt2* gene mutation
10 in *P. digitatum* caused pleiotropic effects, including the reduction of fungal
11 growth and virulence, while its constitutive expression had no phenotypic effect.
12 The *Pdpmt2* null mutants also showed a distinctive colourless phenotype with a
13 strong reduction in the number of conidia, which was associated with severe
14 alterations in the development of conidiophores. Additional effects of the
15 *Pdpmt2* mutation were hyphal morphological alterations, increased sensitivity to
16 cell wall-interfering compounds, and a blockage of invasive growth. In contrast,
17 the *Pdpmt2* mutation increased tolerance to oxidative stress and to the
18 antifungal activity of PAF26. These data confirm the role of protein O-
19 glycosylation in the PAF26-mediated antifungal mechanism present in distant
20 fungal species. Important to future crop protection strategies, this study
21 demonstrates that a mutation rendering fungi more resistant to an antifungal
22 peptide results in severe deleterious effects on fungal growth and virulence.

23 INTRODUCTION

24 Protein glycosylation is a post-translational modification conserved in
25 organisms from yeasts to humans (Lehle *et al.*, 2006). The modification consists
26 of the attachment of different glycan structures to specific proteins, either at an
27 asparagine residue (N-glycosylation) or at serine or threonine residues (O-
28 glycosylation). In fungi, protein glycosylation contributes to the function of
29 proteins involved in important processes such as cell wall (CW) integrity,
30 sensing environmental signals, morphogenesis and the virulence of fungal
31 pathogens (Gentzsch and Tanner, 1996; Prill *et al.*, 2005; Olson *et al.*, 2007;
32 Zhou *et al.*, 2007; Fernández-Álvarez *et al.*, 2012).

33 Protein O-mannosyltransferases (Pmts) catalyse the first step in protein O-
34 mannosylation, transferring mannose to the hydroxyl groups of serine/threonine
35 residues in the nascent protein chain at the lumen of the endoplasmic reticulum
36 (Loibl and Strahl, 2013). Pmts have been identified in prokaryotes, fungi and
37 animals but appear to be absent in plants (Girrbach and Strahl, 2003; Loibl and
38 Strahl, 2013), which makes them a potential target for antifungal strategies in
39 plant protection (Fernández-Álvarez *et al.*, 2009; González *et al.*, 2013). In the
40 budding yeast *Saccharomyces cerevisiae* there are six Pmts divided in the
41 Pmt1, Pmt2 and Pmt4 subfamilies, which differ in the number of genes in each
42 and protein substrate specificity (Gentzsch and Tanner, 1996; Girrbach and
43 Strahl, 2003; Loibl and Strahl, 2013). The Pmt1 and Pmt2 subfamilies are
44 redundant, and their members form heterodimers, while Pmt4 is a single
45 member subfamily and acts as a homodimer. The *PMT* genes in *S. cerevisiae*
46 are not individually essential for viability, likely due to gene redundancy,

1
2
3 47 although several combinations of double mutants are lethal (Gentzsch and
4
5 48 Tanner, 1996; Loibl and Strahl, 2013).
6
7

8
9 In the fission yeast *Schizosaccharomyces pombe* or in filamentous fungi
10
11 50 such as *Aspergillus nidulans*, the human pathogen *Aspergillus fumigatus*, or the
12
13 51 plant pathogens *Ustilago maydis* and *Botrytis cinerea*, only one member for
14
15 52 each Pmt subfamily has been identified (Oka *et al.*, 2004; Willer *et al.*, 2005;
16
17 53 Fernández-Álvarez *et al.*, 2009; Goto *et al.*, 2009; Mouyna *et al.*, 2010;
18
19 54 González *et al.*, 2013). Importantly, the *pmt2* subfamily is essential for the
20
21 55 viability of several fungi studied so far. The requirement of *pmt* genes in fungal
22
23 56 pathogenesis is variable and depends on the specific pathosystem. Both *pmt1*
24
25 57 and *pmt4* of the human pathogens *Candida albicans* and *Cryptococcus*
26
27 58 *neoformans* are necessary for virulence to varying degrees (Timpel *et al.*, 1998;
28
29 59 Prill *et al.*, 2005; Olson *et al.*, 2007; Willger *et al.*, 2009). In contrast, mutants in
30
31 60 either *pmt1* or *pmt4* of *A. fumigatus* are as virulent as the parental strain in a
32
33 61 murine model (Zhou *et al.*, 2007; Mouyna *et al.*, 2010). In *U. maydis*, only the
34
35 62 disruption of *pmt4* specifically affected appressorium formation, penetration and
36
37 63 tumour formation in maize, while *pmt1* disruption was dispensable for plant
38
39 64 infection (Fernández-Álvarez *et al.*, 2009). In *B. cinerea*, the three *pmt* genes
40
41 65 including *pmt2* are required for the pathogenesis of different plants and plant
42
43 66 organs (González *et al.*, 2013).
44
45
46
47
48

49 67 *Penicillium digitatum* causes the citrus fruit green mould disease and
50
51 68 contributes up to 5-10 % of postharvest losses in the main fruit tree crop in the
52
53 69 world. *P. digitatum* is a necrotroph and a wound pathogen that requires a pre-
54
55 70 existing injured fruit peel to penetrate and infect. Despite this rather unspecific
56
57
58
59
60

1
2
3 71 infection mechanism, *P. digitatum* exhibits an exquisite and high degree of host
4
5 72 specificity. The most common method to control *P. digitatum* is the postharvest
6
7 73 application of fungicides, but their continued use has a negative impact on
8
9 74 human health and the environment and has increased the appearance of
10
11 75 resistance isolates. The economic interest in *P. digitatum* has promoted the use
12
13 76 of molecular and genetic tools to characterise the fruit-fungus interaction
14
15 77 (González-Candelas *et al.*, 2010; Ballester *et al.*, 2011; Buron-Moles *et al.*,
16
17 78 2012) and fungal pathogenicity (Wang and Li, 2008; Zhang *et al.*, 2013a; Zhang
18
19 79 *et al.*, 2013b; Gandía *et al.*, 2014). These efforts are exemplified in the recent
20
21 80 release of the genome sequence of three strains (Marcet-Houben *et al.*, 2012;
22
23 81 Sun *et al.*, 2013).

24
25
26
27
28 82 Antimicrobial peptides (AMPs) are promising alternatives to control
29
30 83 pathogens in plant protection (Marcos *et al.*, 2008). PAF26 belongs to the
31
32 84 cationic and tryptophan-rich PAF series of synthetic peptides (López-García *et*
33
34 85 *al.*, 2000). PAF26 is a hexapeptide that inhibits the growth of filamentous fungi
35
36 86 including *P. digitatum* and is effective in controlling citrus fruit infection (Muñoz
37
38 87 *et al.*, 2007a). Previous studies with the model fungi *S. cerevisiae* and
39
40 88 *Neurospora crassa* have revealed insights into the mode of PAF26 antifungal
41
42 89 action (Muñoz *et al.*, 2012; Muñoz *et al.*, 2013b). PAF26 is a cell penetrating
43
44 90 antifungal peptide that first interacts with the fungal cell envelope and then
45
46 91 translocates to the cell interior where it kills the fungal cell (reviewed in Muñoz
47
48 92 *et al.*, 2013a). In *S. cerevisiae*, PAF26 treatment induces genes encoding highly
49
50 93 glycosylated CW proteins (López-García *et al.*, 2010), and the disruption of
51
52 94 protein N- and O-glycosylation genes results in enhanced tolerance to PAF26
53
54 95 (Harries *et al.*, 2013).

1
2
3 96 In this study, the identification and characterisation of *pmt* genes from
4
5 97 *P. digitatum* was conducted. One member from each *pmt1*, *pmt2* and *pmt4*
6
7 98 subfamily was identified and shown to be expressed during fungal growth and
8
9 99 citrus infection. The study reports the functional characterisation of *Pdpmt2* in
10
11 100 *P. digitatum* and its requirement for fungal growth, virulence and sensitivity to
12
13 101 PAF26.
14
15
16
17

18 102 **RESULTS**

21 103 **Identification and sequence analysis of Pmts in *P. digitatum***

22
23
24
25 104 The *Pdpmt1* (GenBank accession number KC757712), *Pdpmt2* (KC757713)
26
27 105 and *Pdpmt4* (KC757714) genes each encode a putative protein O-
28
29 106 mannosyltransferase and were identified in a *P. digitatum* genomic library,
30
31 107 similarly to chitin synthase genes (*chs*) (Gandía *et al.*, 2012). The total mRNA
32
33 108 was reverse transcribed, and the corresponding cDNAs were cloned. The
34
35 109 coding sequences of the three genomic sequences and cDNAs show homology
36
37 110 to other fungal Pmt and belong to the Pmt1, 2 and 4 subfamilies, respectively.
38
39 111 BLASTP searches identified the three Pmts in the recently reported *P. digitatum*
40
41 112 genomes (Marcet-Houben *et al.*, 2012). Our deduced PdPmt1 and PdPmt4
42
43 113 proteins contain 937 and 776 amino acid residues and are identical to
44
45 114 PDIG_19890 and PDIG_11480, respectively, which are annotated as putative
46
47 115 protein mannosyltransferases in the *P. digitatum* PHI26 genome. In contrast,
48
49 116 the amino acid sequence of PdPmt2 differed from the annotated PDIG_43220.
50
51 117 Our cDNA analysis found changes in the intron position, explaining the
52
53 118 difference between PDIG_43220 (737 aa) and PdPmt2 (744 aa).
54
55
56
57
58
59
60

1
2
3 119 The assignment of these identified genes as protein O-
4
5 120 mannosyltransferases was further confirmed by phylogenetic re-construction
6
7 121 with homologous fungal genes (Supporting Fig. S1). The predicted amino acid
8
9 122 sequences showed the presence of the two characteristic domains of the Pmt
10
11 123 family (Supporting Fig. S2): the PMT domain required for
12
13
14 124 O-mannosyltransferase activity and the mannosyltransferase IP3 ryanodine
15
16 125 receptor domain (MIR) composed of three sub-motifs. In addition, the three
17
18 126 proteins showed potential N-glycosylation sites, while only the larger PdPmt1
19
20 127 sequence has potential O-glycosylation sites located at the C-terminus.
21
22

23
24 128 Functional complementation was conducted to confirm the identity of the
25
26 129 *Pdpmt* genes. The *S. cerevisiae pmt* mutants, particularly $\Delta pmt2$, have defects
27
28 130 in CW and exhibit increased sensitivity to the chitin binding fluorophore
29
30 131 calcofluor white (CFW) (Harries *et al.*, 2013; Loibl and Strahl, 2013). We tested
31
32 132 whether the *P. digitatum* genes complemented the growth defect in the
33
34 133 presence of CFW in the *S. cerevisiae pmt* mutants. Reliable data were only
35
36 134 obtained with *S. cerevisiae* $\Delta pmt2$ (Fig. 1). *Pdpmt2* restored the growth of this
37
38 135 yeast mutant under induction conditions (the presence of galactose). In
39
40 136 contrast, complementation was not observed in transformants obtained with
41
42 137 *Pdpmt1* or *Pdpmt4*, which demonstrates that *Pdpmt2* is a functional ortholog of
43
44 138 *S. cerevisiae* *PMT2*.
45
46
47
48

49 139 **Characterisation of *Pdpmt* gene expression**

50
51
52
53 140 The changes in *Pdpmt* gene expression were analysed by qRT-PCR during
54
55 141 axenic growth and fungal infection of citrus fruit. The three *pmt* genes were
56
57 142 expressed during growth in liquid PDB and PDA plates. First, the expression
58
59
60

1
2
3 143 among the three *Pdpmt* genes was compared. The absolute quantification of
4
5 144 the molar concentrations of *pmt*-specific cDNAs was conducted. *Pdpmt4*
6
7 145 showed the lowest expression and was used as the reference to quantify the
8
9 146 expression of the other *pmt* genes (Fig. 2A). *Pdpmt1* was the most highly
10
11 147 expressed and was twenty-fold higher than *Pdpmt4* and ten-fold higher than
12
13 148 *Pdpmt2*.

14
15
16
17 149 A statistically significant increase in the *Pdpmt2* and *Pdpmt4* mRNA levels
18
19 150 was observed during submerged growth of mycelium in PDB (Fig. 2B). The
20
21 151 three *pmt* genes were induced during growth on PDA plates (Fig. 2C) in
22
23 152 correlation with the production of conidia, which starts at day 2 and reaches
24
25 153 maximum at day 7. The effect on *Pdpmt* expression under osmotic and
26
27 154 oxidative stress conditions was also analysed. Our data indicate a differential
28
29 155 regulation in the three genes since *Pdpmt2* was clearly induced in PDA plates
30
31 156 containing 1 mM H₂O₂ or 1.2 M sorbitol while *Pdpmt1* was repressed (Fig. 2D).
32
33
34
35

36 157 The expression of *pmt* genes during the infection of citrus fruit was
37
38 158 determined in experimental inoculations. Fig. 3 shows the results obtained from
39
40 159 two independent experiments in which fruits from different orchards and
41
42 160 harvesting season were used. None of the three *pmt* genes were detected at
43
44 161 early stages of infection (1 day post-inoculation, dpi). From 2 to 7 dpi, an overall
45
46 162 increase in *Pdpmt2* and *Pdpmt4* mRNA during the infection process was
47
48 163 observed. The induction was more pronounced and statistically significant in
49
50 164 *Pdpmt2*, which reached 5-10-fold induction at 7 dpi (Fig. 3A and B). This
51
52 165 induction correlated with conidia production on infected fruit, which started at 4-
53
54 166 5 dpi (Fig. 3C).
55
56
57
58
59
60

1
2
3 167 **Disruption and constitutive expression of *Pdpmt2* in *P. digitatum***
4

5
6 168 Our gene expression results show that *Pdpmt2* is the most responsive of the
7
8 169 three *pmt* genes during axenic growth and infection progress. To characterise
9
10 170 the functional roles of *Pdpmt2*, we generated *P. digitatum* gene disruption and
11
12 171 constitutive expression mutants using *Agrobacterium tumefaciens*-mediated
13
14 172 transformation (ATMT).
15
16

17
18 173 Gene disruption by homologous recombination was conducted using the
19
20 174 pGKO2 vector (Khang *et al.*, 2006) that contains the HSVtk gene as a negative
21
22 175 marker to favour the selection of homologous recombinants (Fig. S3). Four
23
24 176 independent transformants (PDEH508, PDEH510, PDEH515 and PDE525) with
25
26 177 a distinctive phenotype were obtained (see Fig. 4A below). The detailed
27
28 178 characterization of transformant PDEH515 is shown (Fig. S3). PDEH515
29
30 179 underwent a homologous recombination event at the *Pdpmt2* locus as
31
32 180 demonstrated by Southern blot and PCR analyses. As the internal negative
33
34 181 control in further experiments, we selected one transformant (PDEH540) with
35
36 182 an ectopic integration of the T-DNA.
37
38
39
40

41 183 We obtained transformants for *Pdpmt2* constitutive expression under the
42
43 184 strong *gpdA* promoter from *A. nidulans*. Three of them (PDEH58, PDEH59 and
44
45 185 PDEH67) were selected for further analysis (Fig. S4). Southern hybridisation
46
47 186 showed that PDEH59 is a transformant that harbours multiple copies of the
48
49 187 constitutive expression construct. Gene expression studies confirmed that the
50
51 188 null PDEH515 mutant did not express *Pdpmt2*; however, PDEH59 displayed
52
53 189 six-fold increased expression compared with the parental strain (Fig. S5).
54
55
56
57
58
59
60

1
2
3 190 **The *Pdpmt2* mutation results in growth defects and conidiation deficiency**
4
5 191 **in *P. digitatum***
6
7

8 192 The *Pdpmt2* mutation affected *P. digitatum* colony morphology (Fig. 4). The
9
10 193 mutants showed a white fungal colony contrasting with the typical olive green
11
12 194 colour exhibited by the parental strain (Fig. 4A) and grew significantly slower,
13
14 195 reaching only ~40 % of the parental diameter (Fig. 4B). This growth defect was
15
16 196 almost completely reversed by osmotic stabilisation with 1 M sorbitol (Fig. 4B).
17
18 197 In addition, mutants displayed a “fluffy” phenotype, with white cotton-like
19
20 198 masses of vegetative cells that suggest conidiation defects. The production of
21
22 199 conidia from PDEH515 was severely reduced by three orders of magnitude
23
24 200 (Fig. 4C), and obtaining sufficient conidia to perform our experiments was
25
26 201 difficult; therefore, 10-12 plates had to be pooled each time. Moreover, the
27
28 202 concentrated PDEH515 conidia solutions appeared colourless, and conidia
29
30 203 viability dropped much quicker than the parental strain (data not shown).
31
32 204 Interestingly, the conidiation defect was not recovered when PDEH515 was
33
34 205 grown under osmotic stabilization (Fig. 4C).
35
36
37
38
39

40 206 Due to these phenotypes, we characterised the morphology of PDEH515 by
41
42 207 fluorescence microscopy after CFW staining. At early stages of germ tube
43
44 208 elongation, the PDEH515 mutant presented more septa, which were intensively
45
46 209 stained and had shorter interseptal distances than PHI26 (Fig. 5A). The
47
48 210 PDEH515 mutant also showed defects in polarity as demonstrated by tip
49
50 211 dichotomous branching. Older mycelium (24 or 48 h) showed short interseptal
51
52 212 distances that presented intense CFW staining (Fig. 5B), and dichotomous
53
54
55
56
57
58
59
60

1
2
3 213 apical ends, in which the presence of CW thickening and globular balloon-like
4
5 214 structures was common (see higher magnification images in Fig. 5B).
6
7

8 215 The conidiophore structure formed by PDEH515 was also abnormal (Fig.
9
10 216 5C). Typical phialides (p, Fig. 5C) above metulae (m) observed in the PHI26
11
12 217 strain were difficult to distinguish in the mutant. PDEH515 only showed cells
13
14 218 resembling elongated phialides at a number lower than the parental strain.
15
16 219 Putative phialides had at most 1-2 small round cells at the tip with intense CFW
17
18 220 staining, which likely correspond to the few conidia produced by this mutant. In
19
20 221 PDEH515, the long conidia strings common in the parental strain were not
21
22 222 observed. The microscopy characterisation of the constitutive expressors and
23
24 223 the PDEH540 transformant did not reveal any of these defects (data not
25
26 224 shown). Overall, these results demonstrate that *Pdpmt2* is required for normal
27
28 225 mycelial growth and conidiation in *P. digitatum*.
29
30
31
32
33

34 226 **Effects of the *Pdpmt2* deletion on the sensitivity of PDEH515 to diverse** 35 36 227 **compounds and stresses** 37 38

39 228 We examined the sensitivity of the transformants to different compounds.
40
41 229 PDEH515 had increased sensitivity to CW-damaging agents such as CFW or
42
43 230 Congo red (CR) and to the cell membrane destabilising compound sodium
44
45 231 dodecyl sulphate (SDS), indicating a defective CW (Fig. S6). None of the
46
47 232 constitutive expression transformants showed changes in susceptibility to these
48
49 233 compounds (data not shown).
50
51
52

53 234 The $\Delta pmt2$ mutant of *S. cerevisiae* is tolerant to the antifungal peptide
54
55 235 PAF26 (Harries *et al.*, 2013). The sensitivity of *Pdpmt2* transformants to PAF26
56
57
58
59
60

1
2
3 236 activity was tested in two different assays (Fig. 6). PDEH515 was able to grow
4
5 237 on agarose solid medium containing 32 μM PAF26, while the parental strain
6
7 238 and the constitutive expressors were not able to grow on this medium (Fig. 6A).
8
9 239 Dose-response curves in liquid culture confirmed the higher tolerance of
10
11 240 PDEH515 (Fig. 6B). Specifically, PAF26 had an IC_{50} of 1.8 μM and a minimal
12
13 241 inhibitory concentration (MIC) of 4 μM against the parental strain, while PAF26
14
15 242 concentrations as high as 32 μM did not reduce PDEH515 growth after 48 h of
16
17 243 culture.
18
19
20
21

22 244 ***Pdpmt2* is required for *P. digitatum* full virulence against citrus fruit**

23
24

25 245 Fruit inoculation assays were performed to analyse the role of *Pdpmt2* in
26
27 246 pathogenicity and virulence. At a high inoculum dose (10^5 conidia mL^{-1} , Fig.
28
29 247 S7), the incidence of infected wounds inoculated with PHI26 increased along
30
31 248 time and reached 100 % at 5 dpi. The PDEH540, PDEH59 and PDEH67 strains
32
33 249 did not differ significantly from PHI26 in the infection incidence, rate of
34
35 250 progression of maceration area and sporulation. However, the *Pdpmt2* deletion
36
37 251 mutant PDEH515 showed a clear delay in disease progression compared with
38
39 252 the other strains. The reduction of disease incidence on fruits infected with
40
41 253 PDEH515 was more evident at a lower inoculum dose (10^4 conidia mL^{-1}) (Fig.
42
43 254 7). In this case, the incidence of disease caused by PHI26 reached only ~70 %
44
45 255 at 7 dpi, while PDEH515 inoculation resulted in just ~10 % of infected wounds.
46
47 256 Lesion diameter measurements evidenced that at early infection (i.e., 2-5 dpi),
48
49 257 PDEH515 lesions enlarged slower than the rest of the strains (Fig. 7B and
50
51 258 S7B). Significantly, none of the PDEH515-infected wounds showed the typical
52
53 259 colouration of the green mould caused by *P. digitatum* (Fig. 7C and S7D). The
54
55
56
57
58
59
60

1
2
3 260 appearance of white mycelium was rare in the case of PDEH515, and infection
4
5 261 was only noticeable by tissue maceration, even in lesions of size comparable
6
7 262 with the lesions caused by PHI26 (Fig. 7C).
8
9

10 263 We explored additional properties of PDEH515 that may be related to the
11
12 264 plant-pathogen interaction. Reactive oxygen species (ROS) are produced by
13
14 265 plant tissues in response to pathogen infection. PDEH515 grew better than the
15
16 266 parental strain and the other transformants in the presence of hydrogen
17
18 267 peroxide (H₂O₂) (Fig. 8). Consistent with a role in mediating oxidative stress, the
19
20 268 multicopy constitutive expressor PDEH59 had increased susceptibility to H₂O₂.
21
22
23

24 269 An assay for penetration through cellophane membranes (Prados Rosales
25
26 270 and Di Pietro, 2008) was used to test the invasive growth capacity of PDEH515
27
28 271 (Fig. 9). Growth of the parental PHI26 strain on the membranes for 3 days was
29
30 272 sufficient to allow penetration through the membranes and the invasion of the
31
32 273 PDA underneath. In contrast, the PDEH515 mutant was unable to penetrate
33
34 274 cellophane membranes even after 7 days of growth, demonstrating a blockage
35
36 275 of invasive growth capacity.
37
38
39

40 41 42 276 **DISCUSSION**

43
44
45 277 This study reports the identification of one member of each *pmt* subfamily in
46
47 278 the postharvest pathogen *P. digitatum*, consistent with reports that showed the
48
49 279 existence of only one ortholog for each *pmt* subfamily in other filamentous fungi
50
51 280 and in the fission yeast. Functional analysis by complementation of yeast Δpmt
52
53 281 mutants demonstrated that *PdPmt2* is orthologous to *PMT2* from *S. cerevisiae*.
54
55 282 Both *Pmt2* proteins from *P. digitatum* and *S. cerevisiae* have 52 % amino acid
56
57
58
59
60

1
2
3 283 identity, the highest identity value between any *Pmt* from these two fungi. This
4
5 284 is the first study that complements a yeast $\Delta pmt2$ mutant and uses CFW
6
7 285 sensitivity as a complementation assay. Previous heterologous
8
9 286 complementation had been demonstrated for *CaPMT1* in the $\Delta pmt1$ mutant of
10
11 287 *S. cerevisiae* (Timpel *et al.*, 1998) and for *pmt1* and *pmt4* *U. maydis* genes in *S.*
12
13 288 *pombe* (Fernández-Álvarez *et al.*, 2009). Overall, these findings confirm the
14
15 289 functional conservation within each subfamily of *pmt* genes among distantly
16
17 290 related fungi.
18
19
20

21
22 291 Detailed characterisation of fungal *pmt* gene expression has been previously
23
24 292 described in *A. nidulans* (Oka *et al.*, 2004; Goto *et al.*, 2009), *C. neoformans*
25
26 293 (Willger *et al.*, 2009), *B. cinerea* (González *et al.*, 2013) and the yeast *C.*
27
28 294 *albicans* (Timpel *et al.*, 2000; Prill *et al.*, 2005). Overall, the three *pmt*
29
30 295 subfamilies are all expressed under different growth conditions as is also the
31
32 296 case in *P. digitatum*. Our study adds the comparison of gene expression among
33
34 297 the three *Pdpmt*, which demonstrated that *Pdpmt1* has the highest expression,
35
36 298 one order of magnitude higher than *Pdpmt2* or *Pdpmt4*. Our data also indicate
37
38 299 that differential regulation of the three *Pdpmt* genes exists. For example,
39
40 300 *Pdpmt2* is the most responsive of the three and is induced during submerged
41
42 301 and aerial growth, after osmotic and oxidative stresses, and during fungal
43
44 302 infection. In contrast, the *pmt4* gene of *B. cinerea* is the most induced during
45
46 303 tomato leave infection, while *pmt2* remains constant or even declines (González
47
48 304 *et al.*, 2013). In spite of its high induction, the *pmt2* deletion in PDEH515 was
49
50 305 not compensated by the overexpression of any of the other two genes (Fig. S5),
51
52 306 similarly to the findings in the *C. neoformans pmt1* and *pmt4* mutants (Willger *et*
53
54 307 *al.*, 2009).
55
56
57
58
59
60

1
2
3 308 **The *Pdpmt2* gene is necessary for growth, conidiogenesis and cell wall**
4
5 309 **integrity**
6
7

8 310 This study demonstrates that the disruption of *pmt2* has a viable phenotype
9
10 311 in *P. digitatum*. Viable mutants of the Pmt2 subfamily have also been described
11
12 312 in *A. nidulans*, *Aspergillus awamori*, *B. cinerea* and *C. neoformans* (Oka *et al.*,
13
14 313 2004; Oka *et al.*, 2005; Kriangkripiat and Momany, 2009; González *et al.*,
15
16 314 2013; Shimizu *et al.*, 2014). In the pathogens *C. albicans*, *A. fumigatus*, and *U.*
17
18 315 *maydis*, *pmt2* appears to be an essential gene; therefore, the functional
19
20 316 significance of null mutations could not be assayed (Prill *et al.*, 2005; Willger *et*
21
22 317 *al.*, 2009; Mouyna *et al.*, 2010). The selection of transformants in our study
23
24 318 required osmotic stabilisation likely due to the compromised CW integrity of the
25
26 319 mutants. Functional complementation of PDEH515 with the native *Pdpmt2*
27
28 320 could not be demonstrated because of its low conidia recovery and defective
29
30 321 CW, which made the ATMT of this strain not possible after several attempts
31
32 322 (data not shown).
33
34
35
36
37

38 323 The PDEH515 mutant displayed a reduction in radial growth and severe
39
40 324 morphological defects. Significantly, young germlings showed dichotomous tip
41
42 325 branching, suggesting defects in polarity. Early characterisation of polarity
43
44 326 mutants in fungi identified *pmt* genes, as it was the case of the *swaA* mutant in
45
46 327 *A. nidulans* (Shaw and Momany, 2002). The reduction of *pmt2* expression in *A.*
47
48 328 *fumigatus* also demonstrated the involvement of this gene in hyphal polarity
49
50 329 (Fang *et al.*, 2010).
51
52
53

54 330 The $\Delta pmtA$ mutants of *A. nidulans* and *A. awamori* also presented growth
55
56 331 reduction and defects in mycelium morphology with balloon-like structures (Oka
57
58
59
60

1
2
3 332 et al., 2004; Oka et al., 2005), similar to our observations with PDEH515. These
4
5 333 globular structures have also been described in null chitin synthase gene
6
7 334 mutants involved in fungal CW synthesis (Martín-Urdíroz *et al.*, 2008; Gandía et
8
9 335 al., 2014). These morphological defects reveal abnormal CW synthesis,
10
11 336 producing cell enlargements with altered chitin content. The PDEH515 mutant
12
13 337 showed high sensitivity to compounds that target the CW, and the growth defect
14
15 338 was reversed with the addition of sorbitol. Studies have revealed that defective
16
17 339 protein glycosylation has a negative impact on the sensitivity to CW-interfering
18
19 340 compounds and CW integrity, which is restored with the addition of osmotic
20
21 341 stabilisers (Gentzsch and Tanner, 1996; Goto et al., 2009; Kriangkripiat and
22
23 342 Momany, 2009; Mouyna et al., 2010; González et al., 2013). Our gene
24
25 343 expression analysis demonstrated the induction of *Pdpmt2* and *Pdpmt4*
26
27 344 expression under osmotic stress (Fig. 3C) and the repression of *chs* genes
28
29 345 (Gandía et al., 2012), indicating that the CW is remodelled under osmotic
30
31 346 adaptation, which is likely related to the restoration of PDEH515 growth in the
32
33 347 presence of sorbitol.
34
35
36
37
38

39 348 A distinguishable phenotypic characteristic of the PDEH515 mutant was the
40
41 349 white colony associated with reduced conidiation and abnormal development of
42
43 350 conidiophores. A high induction of *Pdpmt2* was observed during conditions that
44
45 351 produce high conidiation such as growth on PDA plates and fruit infection (Fig.
46
47 352 3B and 4). Studies in *A. nidulans* and *A. fumigatus* have also demonstrated a
48
49 353 reduction of conidia in *pmt* mutants (Goto et al., 2009; Kriangkripiat and
50
51 354 Momany, 2009; Fang et al., 2010; Mouyna et al., 2010). A more extreme
52
53 355 phenotype was found in the *B. cinerea* $\Delta pmt2$, which was reported to be
54
55 356 completely unable to sporulate (González et al., 2013). The *wetA* mutants of *A.*
56
57
58
59
60

1
2
3 357 *nidulans* and *P. chrysogenum* also produce colourless and unstable conidia
4
5 358 (Prade and Timberlake, 1994). WetA is a key protein in the regulatory pathway
6
7 359 of conidiation and also a serine and threonine-rich (STR) protein with numerous
8
9 360 potential O-glycosylation sites. Potentially, the conidiation-related phenotype of
10
11 361 PDEH515 could be at least partially a consequence of abnormal WetA
12
13 362 glycosylation and function, which affect conidia development. The alteration of
14
15 363 PDEH515 conidiophore structure at the very early stages of development (Fig.
16
17
18 364 6C) supports a regulatory effect.

21 22 365 **Involvement of *Pmt* in the virulence of *P. digitatum* on citrus fruit**

23
24
25 366 The O-glycosylation of proteins has been linked to the virulence of fungal
26
27 367 pathogens of humans and plants (Lengeler *et al.*, 2008; Fernández-Álvarez *et*
28
29 368 *al.*, 2009). The involvement of *pmt* genes in fungal pathogenesis depends on
30
31 369 the specific fungus-host interaction. However, most of the null mutants in *pmt*
32
33 370 genes whose pathogenesis has been studied belong to the *Pmt1/Pmt4*
34
35 371 subfamilies, due to the difficulties in obtaining viable *pmt2* mutants. We have
36
37 372 shown that *Pdpmt2* disruption produces a reduction in virulence and no
38
39 373 conidiation on fully infected oranges. The *B. cinerea* $\Delta Bcpmt2$ mutant displayed
40
41 374 reduced growth and no conidiation in axenic culture as well as defects in the
42
43 375 adhesion and penetration to host tissue that are associated with reduced
44
45 376 virulence (González *et al.*, 2013). Defective cellular adhesion was also found in
46
47 377 the $\Delta pmt4$ mutant of *U. maydis* (Fernández-Álvarez *et al.*, 2012).

48
49
50
51
52
53 378 The slow growth and defective CW of PDEH515 surely limits fruit tissue
54
55 379 colonisation and explains the decrease in virulence. However, the severe
56
57 380 reduction of virulence and absence of visible hyphal development on fruit also
58
59
60

1
2
3 381 indicate that additional factors may be involved. The production of ROS in
4
5 382 infected citrus fruit is a well characterised host defence response that is
6
7 383 suppressed by *P. digitatum* during infection (Macarisin *et al.*, 2007). Indeed, our
8
9 384 data revealed that *Pdpmt* genes are induced by H₂O₂ and indicate that the
10
11 385 absence of any of these genes would reduce fitness under oxidative stress.
12
13 386 Unexpectedly, the contrary result was found, and *Pdpmt2* disruption produced a
14
15 387 slight increase in tolerance to ROS that goes against an involvement of ROS in
16
17 388 the reduction of virulence of the PDEH515 mutant. Similarly, the inhibition of
18
19 389 plant ROS production did not restore pathogenicity of the *U. maydis* $\Delta pmt4$
20
21 390 mutant in maize (Fernández-Álvarez *et al.*, 2009).
22
23
24
25

26 391 Most sensor proteins from MAPK (mitogen activated protein kinase)
27
28 392 signalling cascades are cell surface proteins that are glycosylated (Rispaill *et al.*,
29
30 393 2009; Lien *et al.*, 2013). In fungal pathogens, MAPK pathways control
31
32 394 morphogenesis, disease progression and virulence (Román *et al.*, 2007). Not
33
34 395 surprisingly, the defective glycosylation of sensor proteins affects the
35
36 396 pathogenesis of fungal plant pathogens. Msb2 is a STR sensor protein in the
37
38 397 high osmolarity glycerol (HOG) pathway, and its defective glycosylation
39
40 398 activates the pathway constitutively (Tatebayashi *et al.*, 2007; Yang *et al.*,
41
42 399 2009). In *P. digitatum*, null mutants of the MAPK Os2/Hog1 have reduced
43
44 400 virulence, indicating that a functional HOG pathway is required for full infection
45
46 401 capacity (Wang *et al.*, 2014). The *U. maydis* $\Delta pmt4$ mutant produced defects in
47
48 402 the glycosylation of Msb2, which in this fungus also activates a MAPK involved
49
50 403 in appressorium formation (Fernández-Álvarez *et al.*, 2012). Msb2 also signals
51
52 404 the filamentous and invasive growth pathway in fungi (Román *et al.*, 2007) and
53
54 405 is necessary for the invasive growth and pathogenesis of *F. oxysporum* on
55
56
57
58
59
60

1
2
3 406 tomato plants (Pérez-Nadales and Di Pietro, 2011). Invasive growth was
4
5 407 completely blocked in the *P. digitatum pmt2* mutant, thus providing additional
6
7 408 reasons to explain the reduction of virulence.
8
9

10
11 409 Future work will aim to identify the specific CW and surface sensor proteins
12
13 410 that are O-glycosylated by PdPmt2 in *P. digitatum* and analyse its involvement
14
15 411 in morphogenesis, sensitivity to PAF peptides and pathogenesis as well as the
16
17 412 cross-talk among these processes.
18
19

20
21 413 **Protein glycosylation genes determine the activity of PAF26 against *P.***
22
23 414 ***digitatum* and *S. cerevisiae***
24
25

26 415 In this study, we demonstrated that PDEH515 conidia are tolerant to PAF26.
27
28 416 Our previous results with *S. cerevisiae* showed enhanced tolerance to PAF26 in
29
30 417 several deletion mutants of protein glycosylation genes, including *PMT1-6*
31
32 418 (Harries *et al.*, 2013). The resistance to PAF26 in *S. cerevisiae* and *P. digitatum*
33
34 419 *pmt2* mutants demonstrates that protein O-glycosylation has a role in the
35
36 420 antifungal action of this peptide that is conserved between distantly related
37
38 421 fungi. Previous studies, mostly conducted in yeast, have found tolerance to
39
40 422 other antifungal peptides and proteins in protein glycosylation mutants (Ibeas *et*
41
42 423 *al.*, 2000; Koo *et al.*, 2004; Harris *et al.*, 2009), demonstrating that proper
43
44 424 protein glycosylation is required for full activity of a number of antifungal
45
46 425 peptides and proteins, including PAF26.
47
48
49
50

51 426 Glycan patterns from CW proteins are proposed to act as docking moieties
52
53 427 for the binding (and therefore activity) of antifungal peptides (Harris *et al.*, 2009;
54
55 428 Marcos and Gandía, 2009). The deletion of the glycosylated highly abundant
56
57
58
59
60

1
2
3 429 CW protein Flo11 abolished the binding of PAF26 to wine “flor” strains of yeast,
4
5 430 which supports this view (Bou Zeidan *et al.*, 2013). The glycosylated domain of
6
7 431 Msb2 from *C. albicans* is capable of binding to the antifungal peptides histatin 5
8
9 432 and LL-37, and its release into the medium protects cells by sequestering the
10
11 433 peptide (Szafranski-Schneider *et al.*, 2012). PAF104 is a heptapeptide derived
12
13 434 from extension of the PAF26 sequence (Muñoz *et al.*, 2007b) that specifically
14
15 435 blocks appressorium formation and reduces virulence in the rice blast pathogen
16
17 436 *Magnaporthe oryzae* (Rebollar and López-García, 2013). PAF104 represses the
18
19 437 expression of *Momsb2*, which encodes the glycosylated Msb2 and is involved in
20
21 438 the Pmk1/Kss1 MAPK pathway that regulates appressorium formation in *M.*
22
23 439 *oryzae* (Liu *et al.*, 2011), demonstrating that PAF peptides affect a MAPK
24
25 440 pathway involved in a plant-pathogen interaction, fungal penetration and
26
27 441 infection. Small antifungal proteins and peptides activate MAPK stress
28
29 442 signalling pathways as a response to their antifungal action (Hayes *et al.*, 2014);
30
31 443 however, whether PAF26 binding to the cell surface influences the activity of the
32
33 444 glycosylated Msb2 and/or MAPK pathways in *P. digitatum* remains unknown.
34
35
36
37
38

39 445 In summary, this study shows the critical role of *Pdpmt2* for growth,
40
41 446 conidiation and virulence of *P. digitatum* and demonstrates that *Pdpmt2*
42
43 447 determines the susceptibility to antifungal peptides exemplified by PAF26.
44
45 448 Therefore, a gene mutation that increases resistance to an antifungal
46
47 449 compound results in detrimental effects to fungal fitness and virulence. This
48
49 450 observation is relevant for the future use of antifungal peptides in crop
50
51 451 protection.
52
53
54
55
56
57
58
59
60

452 **EXPERIMENTAL PROCEDURES**

453 **Fungal strains and culture conditions**

454 The parental strain used was the wild type *Penicillium digitatum* PHI26
455 (CECT20796), whose genome sequence is available (Marcet-Houben *et al.*,
456 2012) (WGS project AKCT01). *P. digitatum* strains were grown at 24 °C either
457 on potato dextrose agar (PDA) (Difco, #213400) plates or in potato dextrose
458 broth (PDB) (Difco, #254920) with shaking. Conidia were collected from plates.
459 To determine colony growth, 5 µL of 1×10^5 conidia mL⁻¹ were deposited on
460 PDA plates, and the colony diameter was measured. Conidiation was quantified
461 on plates grown for 12 days. Cellophane invasion assays were performed as
462 previously described (Prados Rosales and Di Pietro, 2008) by placing
463 autoclaved cellophane membranes on PDA plates and depositing conidial
464 suspensions on membranes.

465 **Sequence analysis of *Pdpmt* genes**

466 *Pdpmt* coding sequences were obtained from a *P. digitatum* fosmid genomic
467 library (Gandía *et al.*, 2012), and sequenced by chromosome walking. To
468 determine the position and size of the introns in each *Pdpmt*, RNA was
469 extracted from the PHI26 strain as reported (Gandía *et al.*, 2012) and reverse
470 transcribed using SuperScript III reverse transcriptase (Invitrogen, #18080-044)
471 into first-strand cDNA, which was then PCR amplified using specific primer
472 pairs, cloned into pGEM-T (Promega #A1360) and sequenced. All the
473 oligonucleotides used in this work are detailed in Supporting Table S1.

1
2
3 474 **S. cerevisiae complementation assays**
4
5

6 475 Functional complementation assays in the *S. cerevisiae* $\Delta pmt2$ strain were
7
8 476 conducted using the pGREG505 plasmid following the Drag and Drop cloning
9
10 477 system (Jansen *et al.*, 2005). The coding sequences for each *Pdpmt* gene were
11
12 478 amplified from plasmids containing cDNAs using primers designed to place
13
14 479 each *Pdpmt* under the *GAL1* inducible promoter. The pGREG505_PdPmt1,
15
16 480 pGREG505_PdPmt2 and pGREG505_PdPmt4 plasmids derived from
17
18 481 pGREG505 were recovered from the BY4741 yeast strain (*MATa his3 Δ 1*
19
20 482 *leu2 Δ 0 met15 Δ 0 ura Δ 0*) selected on synthetic complete (SC) medium lacking
21
22 483 Leu (SC-Leu) and confirmed by sequencing. The plasmids were transformed in
23
24 484 the genetic background of the $\Delta pmt2$ mutant (BY4741 *pmt2 Δ ::KanMX4*) and
25
26 485 selected in SC-Leu.
27
28
29
30

31 486 Sensitivity assays to CFW (Sigma-Aldrich #F3543) were performed to
32
33 487 determine functional complementation. The transformants were grown over
34
35 488 night in liquid SC-Leu with 2 % glucose at 30 °C. The cultures were refreshed to
36
37 489 an OD₆₀₀ of 0.2, pelleted by centrifugation, washed twice in sterile water and
38
39 490 inoculated in 5 mL of either liquid SC-Leu with 2 % glucose (for *GAL1*
40
41 491 repression) or 2 % galactose (for *GAL1* induction). After 9 h of incubation at 30
42
43 492 °C, the cells were diluted to an OD₆₀₀ of 0.1 and ten-fold serial dilutions were
44
45 493 dotted onto SC-Leu plates containing: (i) 2 % glucose, (ii) 2 % glucose, 12.5 μ g
46
47 494 mL⁻¹ CFW, or (iii) 2 % galactose, 12.5 μ g mL⁻¹ CFW. The plates were incubated
48
49
50
51 495 at 30 °C for 3 days.
52
53
54
55
56
57
58
59
60

496 qRT-PCR analysis

497 To determine the expression of the *Pdpmt* genes, total RNA extraction,
498 reverse transcription and quantitative PCR reactions were performed as
499 reported (Gandía *et al.*, 2012). For expression normalisation, the β -tubulin gene,
500 ribosomal protein L18a, and 18S rRNA were simultaneously used as references
501 as previously described.

502 Construction of plasmid vectors for fungal transformation

503 Genomic DNA was extracted from *P. digitatum* as reported (Marcet-Houben
504 *et al.*, 2012). PCR reactions were performed with specific primers and the
505 AccuPrime High Fidelity polymerase (Invitrogen #12346-086). The *Pdpmt2*
506 disruption construct (pGKO2_*Pdpmt2*) was generated by fusion PCR
507 (Szewczyk *et al.*, 2006) and cloned in the binary vector pGKO2 (Khang *et al.*,
508 2006) (see construct details in Supporting Information Fig. S3). The *Pdpmt2*
509 constitutive expression construct (pBHt2_*Pdpmt2*) was designed with the full
510 length *Pdpmt2* coding sequence obtained by PCR amplification from genomic
511 DNA and cloned under the control of the *A. nidulans* glyceraldehyde
512 triphosphate dehydrogenase (*gpdA*) promoter into vector pBHt2 (Mullins *et al.*,
513 2001) (Supporting Information Fig. S4).

514 *Agrobacterium tumefaciens*-mediated transformation of *P. digitatum*

515 *Agrobacterium tumefaciens*-mediated transformation of *P. digitatum* PHI26
516 was performed as previously described (Mullins *et al.*, 2001; Khang *et al.*, 2006;
517 Michielse *et al.*, 2008; Gandía *et al.*, 2014) with minor modifications. *A.*
518 *tumefaciens* carrying each transformation vector (pGKO2_*Pdpmt2* or

1
2
3 519 pBHt2_Pdpmt2) was induced with 200 μ M acetosyringone. Freshly prepared *A.*
4
5 520 *tumefaciens* and conidia of *P. digitatum* were co-cultured at 24 °C for 2 days on
6
7 521 nitrocellulose filters. The filters were transferred to PDA plates containing 50 μ g
8
9 522 mL^{-1} hygromycin (Invivogen #ant-hm-5). The plates were incubated for 2 days at
10
11 523 24 °C or until Hyg^R colonies appeared. In the case of the disruption construct
12
13 524 (pGKO2_Pdpmt2), the plates containing Hyg^R transformant colonies were
14
15 525 washed with sterile water, and the wash was plated on PDA supplemented with
16
17 526 10 μ M 5-Fluoro-2-deoxyuridine (F2dU) (Sigma-Aldrich #F0503) and incubated
18
19 527 for 2-7 days at 24 °C. F2dU is transformed by the herpes simple virus thiamine
20
21 528 kinase gene (HSV tk) encoded in pGKO2 in a toxic compound for negative
22
23 529 selection against ectopic transformants (Khang *et al.*, 2006). Resistant
24
25 530 transformants were checked for Hyg^R and subjected to monosporic culturing for
26
27 531 molecular analysis.
28
29
30
31
32

33 532 **Molecular characterisation of *P. digitatum* transformants**

34
35
36 533 Genomic DNA was digested with *Eco*RI and analysed by Southern blot
37
38 534 using the non-isotopic digoxigenin-labelling kit (DIG-High Prime DNA Labelling
39
40 535 and Detection Starter Kit II, Roche). Transformants were further confirmed by
41
42 536 PCR with genomic DNA with gene specific primer pairs (see Supporting Figs.
43
44 537 S3 and S4).
45
46
47
48

49 538 **Fluorescence microscopy analyses**

50
51
52 539 The morphology of each fungal strain was visualised with fluorescence
53
54 540 microscopy (microscope E90i, Nikon) after staining with 50 μ g mL^{-1} CFW.
55
56 541 Representative images observed in the 40x objective were captured by the NIS-
57
58
59
60

1
2
3 542 Elements BR v2.3 program (Nikon). For sample preparation and fixation, we
4
5 543 followed previously described methods (Harris *et al.*, 1994).
6
7

8 9 544 **Sensitivity to antifungal compounds**

10
11 545 In total, 5 μ L of serial 10-fold dilutions of 1×10^5 conidia mL^{-1} of *P. digitatum*
12
13 546 strains were inoculated on PDA plates supplemented with CFW, SDS (Sigma-
14
15 547 Aldrich #L4509), CR (Sigma-Aldrich #C6767) or H_2O_2 .
16
17
18

19 548 PAF26 (amino acid sequence RKKWFW) was synthesised and provided at
20
21 549 >95 % purity by GenScript Corporation (Piscataway, NJ, USA). Two types of
22
23 550 assays were used to evaluate the antifungal activity of PAF26 against
24
25 551 *P. digitatum* strains. First, the strains were grown on 25 % (one fourth diluted)
26
27 552 potato dextrose (PD) plates solidified with 1.25 % agarose and supplemented
28
29 553 with either 16 or 32 μ M PAF26. Second, dose response experiments were
30
31 554 conducted in 5 % PDB using a 96-well microtiter plate assay as previously
32
33 555 described (Muñoz *et al.*, 2006).
34
35
36
37
38

39 556 **Infection assays**

40
41
42 557 *P. digitatum* inoculation on freshly harvested orange fruits (*Citrus sinensis*)
43
44 558 and the collection of fruit peel tissue samples were conducted as previously
45
46 559 described (González-Candelas *et al.*, 2010). At different times after inoculation,
47
48 560 the incidence of infected wounds, diameter of lesion and conidiation index were
49
50 561 recorded. Three replicas of five fruits each (four wounds per fruit) were used.
51
52
53
54
55
56
57
58
59
60

562 **ACKNOWLEDGMENTS**

563 This work was funded by grant BIO2012-34381 from the “Ministerio de
564 Economía y Competitividad” (MINECO, Spain); and PROMETEOII/2014/027
565 from “Generalitat Valenciana” (Spain). EH was a recipient of a scholarship
566 within the JAE PRE-DOC program (CSIC, EU FEDER funds). We acknowledge
567 to Dr. Seogchan Kang (The Pennsylvania State University, USA) for the pGKO2
568 and pBht2 plasmids; and Dr. Jose M. Guillamón (IATA-CSIC, Spain) for
569 pGREG505. We acknowledge the excellent technical assistance of M. José
570 Pascual.

571

Proof

572 REFERENCES

- 573 **Ballester, A.R., Lafuente, M.T., Forment, J., Gadea, J., De Vos, R.C.H., Bovy, A.G., et**
574 **al.** (2011) Transcriptomic profiling of citrus fruit peel tissues reveals fundamental
575 effects of phenylpropanoids and ethylene on induced resistance. *Mol. Plant Pathol.*, **12**,
576 879-897.
- 577 **Bou Zeidan, M., Carmona, L., Zara, S. and Marcos, J.F.** (2013) *FLO11* gene is involved in
578 the interaction of flor strains of *Saccharomyces cerevisiae* with a biofilm-promoting
579 synthetic hexapeptide. *Appl. Environ. Microbiol.*, **79**, 2023-2032.
- 580 **Buron-Moles, G., López-Pérez, M., González-Candelas, L., Viñas, I., Teixidó, N., Usall,**
581 **J., et al.** (2012) Use of GFP-tagged strains of *Penicillium digitatum* and *Penicillium*
582 *expansum* to study host-pathogen interactions in oranges and apples. *Int. J. Food*
583 *Microbiol.*, **160**, 162-170.
- 584 **Fang, W., Ding, W., Wang, B., Zhou, H., Ouyang, H., Ming, J., et al.** (2010) Reduced
585 expression of the O-mannosyltransferase 2 (AfPmt2) leads to deficient cell wall and
586 abnormal polarity in *Aspergillus fumigatus*. *Glycobiology*, **20**, 542-552.
- 587 **Fernández-Álvarez, A., Elías-Villalobos, A. and Ibeas, J.I.** (2009) The *O*-
588 mannosyltransferase PMT4 is essential for normal appressorium formation and
589 penetration in *Ustilago maydis*. *Plant Cell*, **21**, 3397-3412.
- 590 **Fernández-Álvarez, A., Marín-Menguiano, M., Lanver, D., Jiménez-Martín, A., Elías-**
591 **Villalobos, A., Pérez-Pulido, A.J., et al.** (2012) Identification of O-mannosylated
592 virulence factors in *Ustilago maydis*. *PLoS Pathog.*, **8**, e1002563.
- 593 **Gandía, M., Harries, E. and Marcos, J.F.** (2012) Identification and characterization of chitin
594 synthase genes in the postharvest citrus fruit pathogen *Penicillium digitatum*. *Fungal*
595 *Biol.*, **116**, 654-664.
- 596 **Gandía, M., Harries, E. and Marcos, J.F.** (2014) The myosin motor domain-containing chitin
597 synthase PdChsVII is required for development, cell wall integrity and virulence in the
598 citrus postharvest pathogen *Penicillium digitatum*. *Fungal Genet. Biol.*, **67**, 58-70.
- 599 **Gentzsch, M. and Tanner, W.** (1996) The PMT gene family: Protein O-glycosylation in
600 *Saccharomyces cerevisiae* is vital. *EMBO J.*, **15**, 5752-5759.
- 601 **Girrbach, V. and Strahl, S.** (2003) Members of the evolutionarily conserved PMT family of
602 protein O-mannosyltransferases form distinct protein complexes among themselves. *J.*
603 *Biol. Chem.*, **278**, 12554-12562.
- 604 **González-Candelas, L., Alamar, S., Sánchez-Torres, P., Zacarías, L. and Marcos, J.F.**
605 (2010) A transcriptomic approach highlights induction of secondary metabolism in citrus
606 fruit in response to *Penicillium digitatum* infection. *BMC Plant Biol.*, **10**, 194.
- 607 **González, M., Brito, N., Frías, M. and González, C.** (2013) *Botrytis cinerea* protein *O*-
608 mannosyltransferases play critical roles in morphogenesis, growth, and virulence. *PLoS*
609 *ONE*, **8**, e65924.
- 610 **Goto, M., Harada, Y., Oka, T., Matsumoto, S., Takegawa, K. and Furukawa, K.** (2009)
611 Protein O-mannosyltransferase B and C support hyphal development and differentiation
612 in *Aspergillus nidulans*. *Eukaryot. Cell*, **8**, 1465.

- 1
2
3 613 **Harries, E., Gandía, M., Carmona, L., Read, N.D., Muñoz, A. and Marcos, J.F.** (2013)
4 614 Genes involved in protein glycosylation determine the sensitivity of *Saccharomyces*
5 615 *cerevisiae* to the cell-penetrating antifungal peptide PAF26. *Fungal Genet. Biol.*, **58-59**,
6 616 105-115.
- 7
8 617 **Harris, M., Mora-Montes, H.M., Gow, N.A.R. and Coote, P.J.** (2009) Loss of
9 618 mannosylphosphate from *Candida albicans* cell wall proteins results in enhanced
10 619 resistance to the inhibitory effect of a cationic antimicrobial peptide via reduced peptide
11 620 binding to the cell surface. *Microbiol. SGM*, **155**, 1058-1070.
- 12
13 621 **Harris, S.D., Morrell, J.L. and Hamer, J.E.** (1994) Identification and characterization of
14 622 *Aspergillus nidulans* mutants defective in cytokinesis. *Genetics*, **136**, 517-532.
- 15
16 623 **Hayes, B.M.E., Anderson, M.A., Traven, A., Van Der Weerden, N.L. and Bleackley,**
17 624 **M.R.** (2014) Activation of stress signalling pathways enhances tolerance of fungi to
18 625 chemical fungicides and antifungal proteins. *Cell. Mol. Life Sci.*, **71**, 2651-2666.
- 19
20 626 **Ibeas, J.I., Lee, H., Damsz, B., Prasad, D.T., Pardo, J.M., Hasegawa, P.M., et al.** (2000)
21 627 Fungal cell wall phosphomannans facilitate the toxic activity of a plant PR-5 protein.
22 628 *Plant J.*, **23**, 375-383.
- 23
24 629 **Jansen, G., Wu, C., Schade, B., Thomas, D.Y. and Whiteway, M.** (2005) Drag & Drop
25 630 cloning in yeast. *Gene*, **344**, 43-51.
- 26
27 631 **Khang, C.H., Park, S.Y., Rho, H.S., Lee, Y.H. and Kang, S.** (2006) Filamentous fungi
28 632 (*Magnaporthe grisea* and *Fusarium oxysporum*). *Meth. Mol. Biol.*, **344**, 403-420.
- 29
30 633 **Koo, J.C., Lee, B., Young, M.E., Koo, S.C., Cooper, J.A., Baek, D., et al.** (2004) Pn-AMP1,
31 634 a plant defense protein, induces actin depolarization in yeasts. *Plant Cell Physiol.*, **45**,
32 635 1669-1680.
- 33
34 636 **Kriangkripipat, T. and Momany, M.** (2009) *Aspergillus nidulans* Protein O-
35 637 Mannosyltransferases play roles in cell wall integrity and developmental patterning.
36 638 *Eukaryot. Cell*, **8**, 1475-1485.
- 37
38 639 **Lehle, L., Strahl, S. and Tanner, W.** (2006) Protein glycosylation, conserved from yeast to
39 640 man: A model organism helps elucidate congenital human diseases. *Angew. Chem. Int.*
40 641 *Ed.*, **45**, 6802-6818.
- 41
42 642 **Lengeler, K., Tielker, D. and Ernst, J.** (2008) Protein- O -mannosyltransferases in virulence
43 643 and development. *Cell. Mol. Life Sci.*, **65**, 528-544.
- 44
45 644 **Lien, E.C., Nagiec, M.J. and Dohlman, H.G.** (2013) Proper protein glycosylation promotes
46 645 mitogen-activated protein kinase signal fidelity. *Biochemistry*, **52**, 115-124.
- 47
48 646 **Liu, W., Zhou, X., Li, G., Li, L., Kong, L., Wang, C., et al.** (2011) Multiple plant surface
49 647 signals are sensed by different mechanisms in the rice blast fungus for appressorium
50 648 formation. *PLoS Pathog.*, **7**, e1001261.
- 51
52 649 **Loibl, M. and Strahl, S.** (2013) Protein O-mannosylation: What we have learned from baker's
53 650 yeast. *Biochim. Biophys. Acta - Mol. Cell Res.*, **1833**, 2438-2446.
- 54
55 651 **López-García, B., Gandía, M., Muñoz, A., Carmona, L. and Marcos, J.F.** (2010) A
56 652 genomic approach highlights common and diverse effects and determinants of
57 653 susceptibility on the yeast *Saccharomyces cerevisiae* exposed to distinct antimicrobial
58 654 peptides. *BMC Microbiol.*, **10**, 289.

- 1
2
3 655 **López-García, B., González-Candelas, L., Pérez-Payá, E. and Marcos, J.F.** (2000)
4 656 Identification and characterization of a hexapeptide with activity against
5 657 phytopathogenic fungi that cause postharvest decay in fruits. *Mol. Plant-Microbe*
6 658 *Interact.*, **13**, 837-846.
- 7
8 659 **Macarisin, D., Cohen, L., Eick, A., Rafael, G., Belausov, E., Wisniewski, M., et al.**
9 660 (2007) *Penicillium digitatum* suppresses production of hydrogen peroxide in host tissue
10 661 during infection of citrus fruit. *Phytopathology*, **97**, 1491-1500.
- 11
12 662 **Marcet-Houben, M., Ballester, A.-R., de la Fuente, B., Harries, E., Marcos, J.F.,**
13 663 **Gonzalez-Candelas, L., et al.** (2012) Genome sequence of the necrotrophic fungus
14 664 *Penicillium digitatum*, the main postharvest pathogen of citrus. *BMC Genomics*, **13**,
15 665 646.
- 16
17 666 **Marcos, J.F. and Gandía, M.** (2009) Antimicrobial peptides: to membranes and beyond.
18 667 *Expert Opin. Drug Discov.*, **4**, 659-671.
- 19
20 668 **Marcos, J.F., Muñoz, A., Pérez-Payá, E., Misra, S. and López-García, B.** (2008)
21 669 Identification and rational design of novel antimicrobial peptides for plant protection.
22 670 *Annu. Rev. Phytopathol.*, **46**, 273-301.
- 23
24 671 **Martín-Urdíroz, M., Roncero, M.I., González-Reyes, J.A. and Ruiz-Roldán, C.** (2008)
25 672 ChsVb, a class VII chitin synthase involved in septation, is critical for pathogenicity in
26 673 *Fusarium oxysporum*. *Eukaryot. Cell*, **7**, 112-121.
- 27
28 674 **Michielse, C.B., Hooykaas, P.J.J., van den Hondel, C.A.M.J. and Ram, A.F.J.** (2008)
29 675 *Agrobacterium*-mediated transformation of the filamentous fungus *Aspergillus awamori*.
30 676 *Nat. Prot.*, **3**, 1671-1678.
- 31
32 677 **Mouyna, I., Kniemeyer, O., Jank, T., Loussert, C., Mellado, E., Aimaniananda, V., et al.**
33 678 (2010) Members of protein O-mannosyltransferase family in *Aspergillus fumigatus*
34 679 differentially affect growth, morphogenesis and viability. *Mol. Microbiol.*, **76**, 1205-
35 680 1221.
- 36
37 681 **Mullins, E.D., Chen, X., Romaine, P., Raina, R., Geiser, D.M. and Kang, S.** (2001)
38 682 *Agrobacterium*-mediated transformation of *Fusarium oxysporum*: An efficient tool for
39 683 insertional mutagenesis and gene transfer. *Phytopathology*, **91**, 173-180.
- 40
41 684 **Muñoz, A., Gandía, M., Harries, E., Carmona, L., Read, N.D. and Marcos, J.F.** (2013a)
42 685 Understanding the mechanism of action of cell-penetrating antifungal peptides using
43 686 the rationally designed hexapeptide PAF26 as a model. *Fungal Biol. Rev.*, **26**, 146-155.
- 44
45 687 **Muñoz, A., Harries, E., Contreras-Valenzuela, A., Carmona, L., Read, N.D. and**
46 688 **Marcos, J.F.** (2013b) Two functional motifs define the interaction, internalization and
47 689 toxicity of the cell-penetrating antifungal peptide PAF26 on fungal cells. *PLoS ONE*, **8**,
48 690 e54813.
- 49
50 691 **Muñoz, A., López-García, B. and Marcos, J.F.** (2006) Studies on the mode of action of the
51 692 antifungal hexapeptide PAF26. *Antimicrob. Agents Chemother.*, **50**, 3847-3855.
- 52
53 693 **Muñoz, A., López-García, B. and Marcos, J.F.** (2007a) Comparative study of antimicrobial
54 694 peptides to control citrus postharvest decay caused by *Penicillium digitatum*. *J. Agric.*
55 695 *Food Chem.*, **55**, 8170-8176.
- 56
57 696 **Muñoz, A., López-García, B., Pérez-Payá, E. and Marcos, J.F.** (2007b) Antimicrobial
58 697 properties of derivatives of the cationic tryptophan-rich hexapeptide PAF26. *Biochem.*
59 698 *Biophys. Res. Commun.*, **354**, 172-177.

- 1
2
3 699 **Muñoz, A., Marcos, J.F. and Read, N.D.** (2012) Concentration-dependent mechanisms of
4 700 cell penetration and killing by the *de novo* designed antifungal hexapeptide PAF26. *Mol.*
5 701 *Microbiol.*, **85**, 89-106.
- 6
7 702 **Oka, T., Hamaguchi, T., Sameshima, Y., Goto, M. and Furukawa, K.** (2004) Molecular
8 703 characterization of protein O-mannosyltransferase and its involvement in cell-wall
9 704 synthesis in *Aspergillus nidulans*. *Microbiology*, **150**, 1973-1982.
- 10
11 705 **Oka, T., Sameshima, Y., Koga, T., Kim, H., Goto, M. and Furukawa, K.** (2005) Protein O-
12 706 mannosyltransferase A of *Aspergillus awamori* is involved in O-mannosylation of
13 707 glucoamylase I. *Microbiology*, **151**, 3657-3667.
- 14
15 708 **Olson, G.M., Fox, D.S., Wang, P., Alspaugh, J.A. and Buchanan, K.L.** (2007) Role of
16 709 protein O-mannosyltransferase Pmt4 in the morphogenesis and virulence of
17 710 *Cryptococcus neoformans*. *Eukaryot. Cell*, **6**, 222-234.
- 18
19 711 **Pérez-Nadales, E. and Di Pietro, A.** (2011) The membrane mucin Msb2 regulates invasive
20 712 growth and plant infection in *Fusarium oxysporum*. *Plant Cell*, **23**, 1171-1185.
- 21
22 713 **Prade, R.A. and Timberlake, W.E.** (1994) The *Penicillium chrysogenum* and *Aspergillus*
23 714 *nidulans wetA* developmental regulatory genes are functionally equivalent. *Molecular*
24 715 *and General Genetics*, **244**, 539-547.
- 25
26 716 **Prados Rosales, R.C. and Di Pietro, A.** (2008) Vegetative hyphal fusion is not essential for
27 717 plant infection by *Fusarium oxysporum*. *Eukaryot. Cell*, **7**, 162-171.
- 28
29 718 **Prill, S.K.H., Klinkert, B., Timpel, C., Gale, C.A., Schroppel, K. and Ernst, J.F.** (2005)
30 719 *PMT* family of *Candida albicans*: five protein mannosyltransferase isoforms affect
31 720 growth, morphogenesis and antifungal resistance. *Mol. Microbiol.*, **55**, 546-560.
- 32
33 721 **Rebollar, A. and López-García, B.** (2013) PAF104, a synthetic peptide to control rice blast
34 722 disease by blocking appressorium formation in *Magnaporthe oryzae*. *Mol. Plant-Microbe*
35 723 *Interact.*, **26**, 1407-1416.
- 36
37 724 **Rispail, N., Soanes, D.M., Ant, C., Czajkowski, R., Grunler, A., Huguet, R., et al.** (2009)
38 725 Comparative genomics of MAP kinase and calcium-calcineurin signalling components in
39 726 plant and human pathogenic fungi. *Fungal Genet. Biol.*, **46**, 287-298.
- 40
41 727 **Román, E., Arana, D.M., Nombela, C., Alonso-Monge, R. and Pla, J.** (2007) MAP kinase
42 728 pathways as regulators of fungal virulence. *Trends Microbiol.*, **15**, 181-190.
- 43
44 729 **Shaw, B.D. and Momany, M.** (2002) *Aspergillus nidulans* polarity mutant *swaA* is
45 730 complemented by protein O-mannosyltransferase *pmtA*. *Fungal Genet. Biol.*, **37**, 263-
46 731 270.
- 47
48 732 **Shimizu, K., Imanishi, Y., Toh-e, A., Uno, J., Chibana, H., Hull, C.M., et al.** (2014)
49 733 Functional characterization of PMT2, encoding a protein-O-mannosyltransferase, in the
50 734 human pathogen *Cryptococcus neoformans*. *Fungal genetics and biology : FG & B*, **69**,
51 735 13-22.
- 52
53 736 **Sun, X., Ruan, R., Lin, L., Zhu, C., Zhang, T., Wang, M., et al.** (2013) Genomewide
54 737 investigation into DNA elements and ABC transporters involved in imazalil resistance in
55 738 *Penicillium digitatum*. *FEMS Microbiol. Lett.*, **348**, 11-18.
- 56
57 739 **Szafrański-Schneider, E., Swidergall, M., Cottier, F., Tielker, D., Roman, E., Pla, J., et**
58 740 **al.** (2012) Msb2 shedding protects *Candida albicans* against antimicrobial peptides.
59 741 *PLoS Pathog.*, **8**, e1002501.
- 60

- 1
2
3 742 **Szewczyk, E., Nayak, T., Oakley, C.E., Edgerton, H., Xiong, Y., Taheri-Talesh, N., *et al.***
4 743 (2006) Fusion PCR and gene targeting in *Aspergillus nidulans*. *Nat. Protocols*, **1**, 3111-
5 744 3120.
- 6
7 745 **Tatebayashi, K., Tanaka, K., Yang, H.Y., Yamamoto, K., Matsushita, Y., Tomida, T., *et***
8 746 ***al.*** (2007) Transmembrane mucins Hkr1 and Msb2 are putative osmosensors in the
9 747 SHO1 branch of yeast HOG pathway. *EMBO J.*, **26**, 3521-3533.
- 10
11 748 **Timpel, C., Strahl-Bolsinger, S., Ziegelbauer, K. and Ernst, J.F.** (1998) Multiple functions
12 749 of Pmt1p-mediated protein O-mannosylation in the fungal pathogen *Candida albicans*.
13 750 *J. Biol. Chem.*, **273**, 20837-20846.
- 14
15 751 **Timpel, C., Zink, S., Strahl-Bolsinger, S., Schroppel, K. and Ernst, J.** (2000)
16 752 Morphogenesis, adhesive properties, and antifungal resistance depend on the Pmt6
17 753 protein mannosyltransferase in the fungal pathogen *Candida albicans*. *J. Bacteriol.*,
18 754 **182**, 3063-3071.
- 19
20 755 **Wang, J.Y. and Li, H.Y.** (2008) *Agrobacterium tumefaciens*-mediated genetic transformation
21 756 of the phytopathogenic fungus *Penicillium digitatum*. *J. Zhejiang Univ. Sci. B*, **9**, 823-
22 757 828.
- 23
24 758 **Wang, M., Chen, C., Zhu, C., Sun, X., Ruan, R. and Li, H.** (2014) Os2 MAP kinase-
25 759 mediated osmotic stress tolerance in *Penicillium digitatum* is associated with its positive
26 760 regulation on glycerol synthesis and negative regulation on ergosterol synthesis.
27 761 *Microbiol. Res.*, **10.1016/j.micres.2013.12.004**.
- 28
29 762 **Willer, T., Brandl, M., Sipiczki, M. and Strahl, S.** (2005) Protein O-mannosylation is crucial
30 763 for cell wall integrity, septation and viability in fission yeast. *Mol. Microbiol.*, **57**, 156-
31 764 170.
- 32
33 765 **Willger, S.D., Ernst, J.F., Alspaugh, J.A. and Lengeler, K.B.** (2009) Characterization of the
34 766 *PMT* gene family in *Cryptococcus neoformans*. *PLoS ONE*, **4**, e6321.
- 35
36 767 **Yang, H.Y., Tatebayashi, K., Yamamoto, K. and Saito, H.** (2009) Glycosylation defects
37 768 activate filamentous growth Kss1 MAPK and inhibit osmoregulatory Hog1 MAPK. *EMBO*
38 769 *J.*, **28**, 1380-1391.
- 39
40 770 **Zhang, T., Sun, X., Xu, Q., Zhu, C., Li, Q. and Li, H.** (2013a) *PdSNF1*, a sucrose non-
41 771 fermenting protein kinase gene, is required for *Penicillium digitatum* conidiation and
42 772 virulence. *App. Microbiol. Biotech.*, **97**, 5433-5445.
- 43
44 773 **Zhang, T., Xu, Q., Sun, X. and Li, H.** (2013b) The calcineurin-responsive transcription factor
45 774 Crz1 is required for conidiation, full virulence and DMI resistance in *Penicillium*
46 775 *digitatum*. *Microbiol. Res.*, **168**, 211-222.
- 47
48 776 **Zhou, H., Hu, H.Y., Zhang, L.J., Li, R.Y., Ouyang, H.M., Ming, J., *et al.*** (2007) O-
49 777 mannosyltransferase 1 in *Aspergillus fumigatus* (AfPmt1p) is crucial for cell wall
50 778 integrity and conidium morphology, especially at an elevated temperature. *Eukaryot.*
51 779 *Cell*, **6**, 2260-2268.
52 780

781 **FIGURE LEGENDS**

782 **Fig. 1.** Complementation assay of the *S. cerevisiae* $\Delta pmt2$ mutant with the *P.*
783 *digitatum* *Pdpmt* genes. Yeast cells transformed with each pGREG505 plasmid
784 (indicated at the left side) were grown at 30 °C for 9 h in SC-Leu medium
785 containing either 0.2 % glucose (Glu) or 0.2 % galactose (Gal). Serial ten-fold
786 dilutions of these cells at 0.1 OD₆₀₀ were dotted onto SC-Leu plates with Glu or
787 Gal supplemented with 12.5 $\mu\text{g mL}^{-1}$ CFW as indicated and incubated at 30 °C
788 for 3 days. Note that the *S. cerevisiae* $\Delta pmt2$ strain presents high sensitivity to
789 CFW under repression conditions (+ Glu) and that this phenotype is rescued
790 only with *Pdpmt2* under the inductive condition (+ Gal).

791 **Fig. 2.** Quantification of *Pdpmt* gene expression by qRT-PCR. (A) Comparison
792 of *Pdpmt* gene expression after 2 days (d) of growth in PDB. The Ct values
793 obtained by qRT-PCR were transformed to molar amounts of cDNA through
794 equations obtained from standard curves (obtained by amplification of serial
795 two-fold dilutions of equimolar amounts of each *Pdpmt* amplicon) and
796 normalized to the lowest expression of *Pdpmt4* (marked with an inverted
797 triangle). (B) Relative expression of *Pdpmt* genes in submerged culture (PDB)
798 after 1, 2, 3 or 6 d of growth as indicated. (C) Relative expression of *Pdpmt*
799 genes in solid medium (PDA) after 2, 4 or 7 d of growth as indicated. (D)
800 Relative expression of *Pdpmt* genes under oxidative or osmotic stress. Graphs
801 show the relative expression at day 4 of growth in PDA (control) and PDA
802 supplemented with H₂O₂ or sorbitol as indicated. The (B), (C) and (D) graphs
803 show the relative expression normalised independently for each gene to the
804 samples indicated by an inverted triangle. In all graphs, the bars represent the

1
2
3 805 means \pm standard deviations (SD) of three replicates. Statistically significant
4
5 806 differences are labelled with an asterisk ($p < 0.05$).

7
8 807 **Fig. 3.** Relative expression of *Pdpmt* genes during orange fruit infection. (A) and
9
10 808 (B) graphs show the relative expression at each day post-inoculation (dpi) in
11
12 809 two independent experiments. The values were normalised independently for
13
14 810 each gene to the value at 2 dpi. Statistically significant differences are labelled
15
16 811 with an asterisk ($p < 0.05$). (C) Representative images for the progress of fungal
17
18 812 colonisation on infected fruit.

20
21
22 813 **Fig. 4.** Colony morphology and growth of *P. digitatum* parental and mutant
23
24 814 strains. (A) *P. digitatum* strain colonies grown on PDA plates at 24 °C for 7 days
25
26 815 as indicated: parental strain PHI26, mutants PDEH508, PDEH510, PDEH515
27
28 816 and PDEH525, and the ectopic transformant PDEH540. (B) Growth of PHI26
29
30 817 (triangles), PDEH515 (circles) and PDEH540 (squares) on PDA plates (black
31
32 818 symbols and straight lines) and PDA plates supplemented with 1 M sorbitol
33
34 819 (white symbols and stripped lines). Data show the mean \pm SD of three replicas
35
36 820 of the diameter registered daily. (C) Conidia production of PHI26, PDEH515 and
37
38 821 PDEH540 on PDA plates and PDA plates supplemented with 1 M sorbitol. Data
39
40 822 show the mean \pm SD of three replicas of the conidia mL^{-1} produced per plate.

42
43
44
45 823 **Fig. 5.** Comparative fluorescence microscopy analysis of *P. digitatum* PHI26
46
47 824 and PDEH515 strains. (A) Germlings of PHI26 and PDEH515 after 16 h of
48
49 825 incubation at 24 °C of conidial suspension in PDB. (B) Mycelium of PHI26 and
50
51 826 PDEH515 grown on slides. (C) Conidiophore structure formed on slides after
52
53 827 72 h of growth. Images show the DIC bright fields and the corresponding
54
55 828 fluorescence fields of samples stained with CFW to visualize the CW. Letters on
56
57
58
59
60

1
2
3 829 the images indicate the septum (s), the balloon-like structures (b) formed in the
4
5 830 mycelium, and the different cell types of conidiophores; rame (r), metulae (m),
6
7 831 phialide (f) and conidium (c).
8
9

10 **Fig. 6.** Antifungal activity of the PAF26 peptide against *P. digitatum* strains. (A)
11
12 833 In total, 5 μL of three serial five-fold dilutions (2.5×10^4 , 5×10^3 , and 10^3 conidia
13
14 834 mL^{-1} , indicated by the upper triangle) from the parental PHI26, the deletion
15
16
17 835 mutant PDEH515, the ectopic transformant PDEH540 and the two constitutive
18
19 836 transformants PDEH59 and PDEH67 were grown at 24 °C for 7 days on PD
20
21 837 agarose 24-well plates with either no peptide (control) or containing 16 μM or 32
22
23 838 μM PAF32 as indicated. (B) Dose response experiment of the growth of
24
25
26 839 *P. digitatum* PHI26 (grey circles) or PDEH515 (open triangles) exposed to
27
28 840 increasing PAF26 concentrations. The values of triplicate samples are shown.
29
30 841 The values corresponding to PHI26 were adjusted to a four parameter
31
32 842 sigmoidal curve (black line) with 50 % inhibitory concentration (IC_{50}) of 1.8 μM (r
33
34 843 = 0.9553).
35
36
37

38 **Fig. 7.** Virulence assays of *P. digitatum* parental PHI26 or mutant PDEH515 on
39
40 845 orange fruit at low inoculum dose (10^4 conidia mL^{-1}). (A) Incidence of infection
41
42 846 determined as the percentage of infected wounds. (B) Lesion diameter of the
43
44
45 847 infected wounds. In (A) and (B), data show mean value \pm SD of three replicates
46
47 848 (five fruits per replica and four wounds per fruit) at each day post-inoculation
48
49 849 (dpi). (C) Representative images of three oranges infected with each fungal
50
51 850 strain at 7 dpi.
52
53

54
55 **Fig. 8.** Sensitivity of *P. digitatum* strains to hydrogen peroxide. In total, 5 μL of
56
57 852 three serial ten-fold dilutions (10^5 , 10^4 and 10^3 conidia mL^{-1}) of the same strains
58
59
60

1
2
3 853 as in Fig.6 were applied on PDA plates supplemented with three different
4
5 854 concentrations of H₂O₂. The plates were incubated at 24 °C for 4 days.
6
7

8 855 **Fig. 9.** Invasive growth of *P. digitatum* PHI26 parental and PDEH515 mutant
9
10 856 strains. The top diagram shows a scheme to follow the experimental procedure.
11
12 857 In total, 5 µL of 2.5 x 10⁴ conidia mL⁻¹ were grown for 3, 5, or 7 days on PDA
13
14 858 plates covered by a cellophane membrane (A), then the cellophane with the
15
16
17 859 colony was removed (B), and finally the plate was incubated for 4 additional
18
19 860 days (C).
20
21
22 861
23
24
25
26
27
28
29
30
31
32
33
34
35
36
37
38
39
40
41
42
43
44
45
46
47
48
49
50
51
52
53
54
55
56
57
58
59
60

Proof

1
2
3 862 **SUPPORTING INFORMATION**
4

5
6 863 **Supporting Fig. S1.** Phylogenetic analysis of *P. digitatum* PdPmt1, PdPmt2,
7
8 864 PdPmt4 and homologous sequences in fungi.
9

10
11 865 **Supporting Fig. S2.** Domain organisation of Pmt proteins from *P. digitatum*.
12

13
14 866 **Supporting Fig. S3.** Disruption of the *Pdpmt2* gene in *P. digitatum*.
15

16
17
18 867 **Supporting Fig. S4.** Constitutive expression of the *Pdpmt2* gene in *P.*
19
20 868 *digitatum*.
21

22
23 869 **Supporting Fig. S5.** Relative quantification of *Pdpmt* gene expression in the *P.*
24
25 870 *digitatum* strains.
26

27
28
29 871 **Supporting Fig. S6.** Sensitivity of the *P. digitatum* strains to different antifungal
30
31 872 compounds.
32

33
34 873 **Supporting Fig. S7.** Virulence assays on orange fruits of *P. digitatum* strains at
35
36 874 high inoculum dose (10^5 conidia mL⁻¹).
37

38
39
40 875 **Supporting Table S1.** Oligonucleotide primers used in this work.
41
42
43
44
45
46
47
48
49
50
51
52
53
54
55
56
57
58
59
60

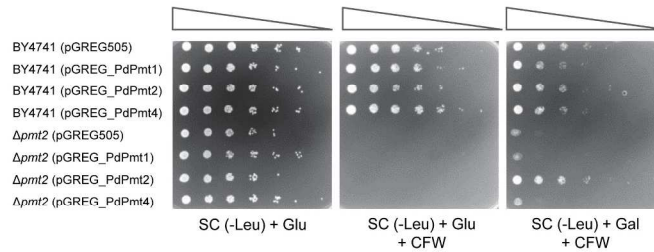
Figure 1 (Harries *et al.*, 2014)

Fig. 1. Complementation assay of the *S. cerevisiae* $\Delta pmt2$ mutant with the *P. digitatum* *Pdpmt* genes. Yeast cells transformed with each pGREG505 plasmid (indicated at the left side) were grown at 30 °C for 9 h in SC-Leu medium containing either 0.2 % glucose (Glu) or 0.2 % galactose (Gal). Serial ten-fold dilutions of these cells at 0.1 OD₆₀₀ were dotted onto SC-Leu plates with Glu or Gal supplemented with 12.5 $\mu\text{g mL}^{-1}$ CFW as indicated and incubated at 30 °C for 3 days. Note that the *S. cerevisiae* $\Delta pmt2$ strain presents high sensitivity to CFW under repression conditions (+ Glu) and that this phenotype is rescued only with *Pdpmt2* under the inductive condition (+ Gal).

190x275mm (300 x 300 DPI)

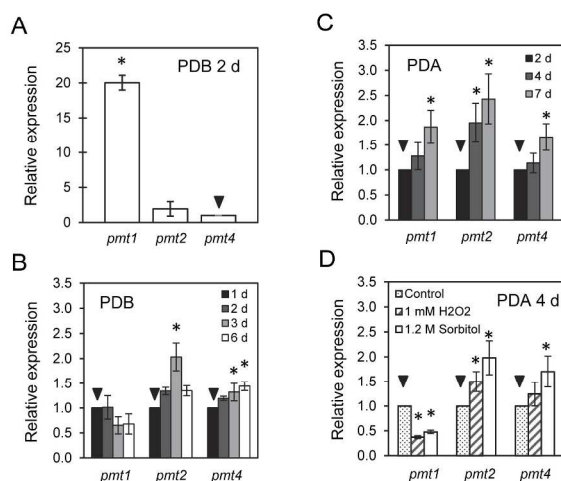
Figure 2 (Harries *et al.*, 2014)

Fig. 2. Quantification of *Pdpmt* gene expression by qRT-PCR. (A) Comparison of *Pdpmt* gene expression after 2 days (d) of growth in PDB. The Ct values obtained by qRT-PCR were transformed to molar amounts of cDNA through equations obtained from standard curves (obtained by amplification of serial two-fold dilutions of equimolar amounts of each *Pdpmt* amplicon) and normalized to the lowest expression of *Pdpmt4* (marked with an inverted triangle). (B) Relative expression of *Pdpmt* genes in submerged culture (PDB) after 1, 2, 3 or 6 d of growth as indicated. (C) Relative expression of *Pdpmt* genes in solid medium (PDA) after 2, 4 or 7 d of growth as indicated. (D) Relative expression of *Pdpmt* genes under oxidative or osmotic stress. Graphs show the relative expression at day 4 of growth in PDA (control) and PDA supplemented with H₂O₂ or sorbitol as indicated. The (B), (C) and (D) graphs show the relative expression normalised independently for each gene to the samples indicated by an inverted triangle. In all graphs, the bars represent the means \pm standard deviations (SD) of three replicates. Statistically significant differences are labelled with an asterisk ($p < 0.05$).

190x275mm (300 x 300 DPI)

1
2
3
4
5
6
7
8
9
10
11
12
13
14
15
16
17
18
19
20
21
22
23
24
25
26
27
28
29
30
31
32
33
34
35
36
37
38
39
40
41
42
43
44
45
46
47
48
49
50
51
52
53
54
55
56
57
58
59
60

Figure 3 (Harries *et al.*, 2014)

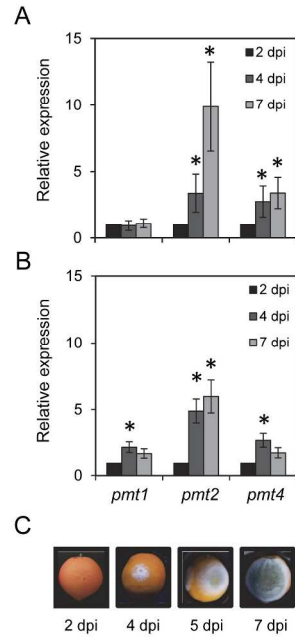


Fig. 3. Relative expression of *Pdpmt* genes during orange fruit infection. (A) and (B) graphs show the relative expression at each day post-inoculation (dpi) in two independent experiments. The values were normalised independently for each gene to the value at 2 dpi. Statistically significant differences are labelled with an asterisk ($p < 0.05$). (C) Representative images for the progress of fungal colonisation on infected fruit.

190x275mm (300 x 300 DPI)

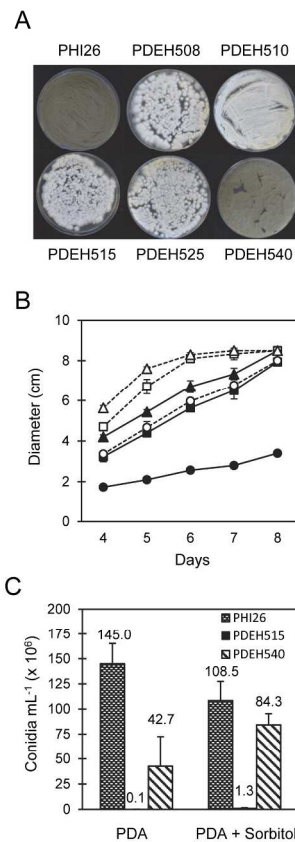
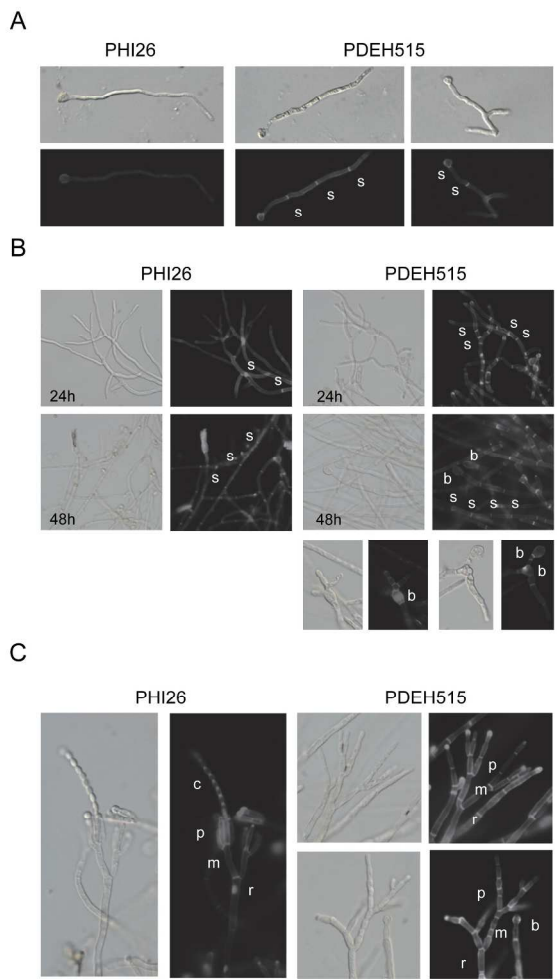
Figure 4 (Harries *et al.*, 2014)

Fig. 4. Colony morphology and growth of *P. digitatum* parental and mutant strains. (A) *P. digitatum* strain colonies grown on PDA plates at 24 °C for 7 days as indicated: parental strain PHI26, mutants PDEH508, PDEH510, PDEH515 and PDEH525, and the ectopic transformant PDEH540. (B) Growth of PHI26 (triangles), PDEH515 (circles) and PDEH540 (squares) on PDA plates (black symbols and straight lines) and PDA plates supplemented with 1 M sorbitol (white symbols and striped lines). Data show the mean \pm SD of three replicas of the diameter registered daily. (C) Conidia production of PHI26, PDEH515 and PDEH540 on PDA plates and PDA plates supplemented with 1 M sorbitol. Data show the mean \pm SD of three replicas of the conidia mL^{-1} produced per plate.

190x275mm (300 x 300 DPI)

1
2
3
4
5
6
7
8
9
10
11
12
13
14
15
16
17
18
19
20
21
22
23
24
25
26
27
28
29
30
31
32
33
34
35
36
37
38
39
40
41
42
43
44
45
46
47
48
49
50
51
52
53
54
55
56
57
58
59
60

Figure 5 (Harries *et al.*, 2014)



190x275mm (300 x 300 DPI)

1
2
3
4
5
6
7
8
9
10
11 **Fig. 5.** Comparative fluorescence microscopy analysis of *P. digitatum* PHI26
12 and PDEH515 strains. (A) Germlings of PHI26 and PDEH515 after 16 h of
13 incubation at 24 °C of conidial suspension in PDB. (B) Mycelium of PHI26 and
14 PDEH515 grown on slides. (C) Conidiophore structure formed on slides after
15 72 h of growth. Images show the DIC bright fields and the corresponding
16 fluorescence fields of samples stained with CFW to visualize the CW. Letters
17 on the images indicate the septum (s), the balloon-like structures (b) formed in
18 the mycelium, and the different cell types of conidiophores; rame (r), metulae
19 (m), phialide (f) and conidium (c).
20
21
22
23
24
25
26
27
28
29
30
31
32
33
34
35
36
37
38
39
40
41
42
43
44
45
46
47
48
49
50
51
52
53
54
55
56
57
58
59
60

190x275mm (300 x 300 DPI)

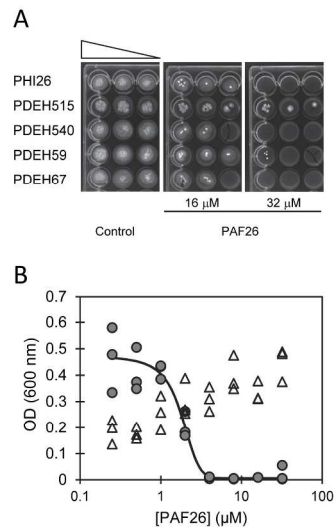
1
2
3
4
5
6
7
8
9
10
11
12
13
14
15
16
17
18
19
20
21
22
23
24
25
26
27
28
29
30
31
32
33
34
35
36
37
38
39
40
41
42
43
44
45
46
47
48
49
50
51
52
53
54
55
56
57
58
59
60Figure 6 (Harries *et al.*, 2014)

Fig. 6. Antifungal activity of the PAF26 peptide against *P. digitatum* strains. (A) In total, 5 μL of three serial five-fold dilutions (2.5×10^4 , 5×10^3 , and 10^3 conidia mL^{-1} , indicated by the upper triangle) from the parental PHI26, the deletion mutant PDEH515, the ectopic transformant PDEH540 and the two constitutive transformants PDEH59 and PDEH67 were grown at 24 $^\circ\text{C}$ for 7 days on PD agarose 24-well plates with either no peptide (control) or containing 16 μM or 32 μM PAF32 as indicated. (B) Dose response experiment of the growth of *P. digitatum* PHI26 (grey circles) or PDEH515 (open triangles) exposed to increasing PAF26 concentrations. The values of triplicate samples are shown. The values corresponding to PHI26 were adjusted to a four parameter sigmoidal curve (black line) with 50 % inhibitory concentration (IC_{50}) of 1.8 μM ($r = 0.9553$).

190x275mm (300 x 300 DPI)

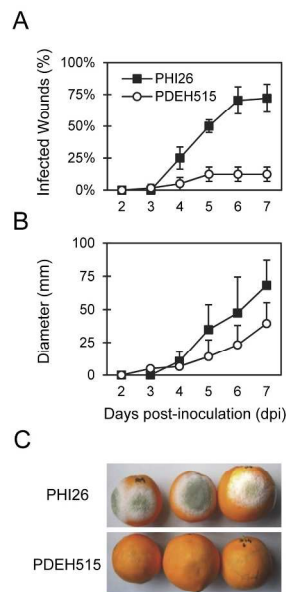
Figure 7 (Harries *et al.*, 2014)

Fig. 7. Virulence assays of *P. digitatum* parental PHI26 or mutant PDEH515 on orange fruit at low inoculum dose (10^4 conidia mL^{-1}). (A) Incidence of infection determined as the percentage of infected wounds. (B) Lesion diameter of the infected wounds. In (A) and (B), data show mean value \pm SD of three replicates (five fruits per replica and four wounds per fruit) at each day post-inoculation (dpi). (C) Representative images of three oranges infected with each fungal strain at 7 dpi.

190x275mm (300 x 300 DPI)

1
2
3
4
5
6
7
8
9
10
11
12
13
14
15
16
17
18
19
20
21
22
23
24
25
26
27
28
29
30
31
32
33
34
35
36
37
38
39
40
41
42
43
44
45
46
47
48
49
50
51
52
53
54
55
56
57
58
59
60

Figure 8 (Harries *et al.*, 2014)

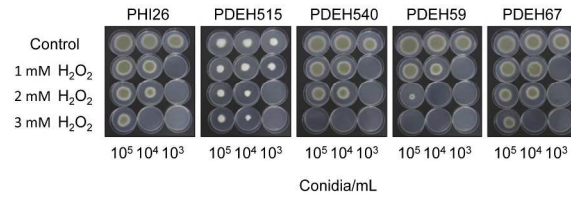


Fig. 8. Sensitivity of *P. digitatum* strains to hydrogen peroxide. In total, 5 μ L of three serial ten-fold dilutions (10^5 , 10^4 and 10^3 conidia mL⁻¹) of the same strains as in Fig.6 were applied on PDA plates supplemented with three different concentrations of H₂O₂. The plates were incubated at 24 °C for 4 days.

190x275mm (300 x 300 DPI)

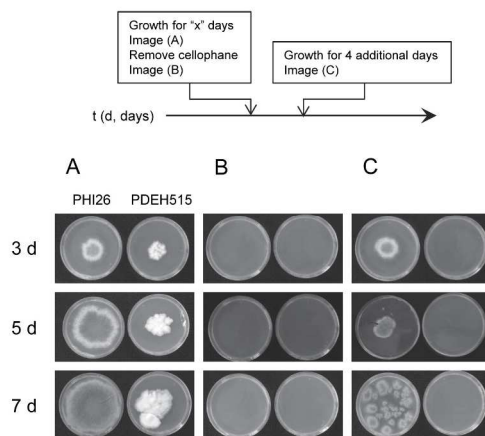
Figure 9 (Harries *et al.*, 2014)

Fig. 9. Invasive growth of *P. digitatum* PHI26 parental and PDEH515 mutant strains. The top diagram shows a scheme to follow the experimental procedure. In total, 5 μL of 2.5×10^4 conidia mL^{-1} were grown for 3, 5, or 7 days on PDA plates covered by a cellophane membrane (A), then the cellophane with the colony was removed (B), and finally the plate was incubated for 4 additional days (C).

190x275mm (300 x 300 DPI)